Study of Resistive Plate Chamber and Scintillators

Experimental Project I : REPORT

submitted by
Anil Kumar
Research Scholar, INO, TIFR

under the supervision of
Prof. Gobinda Majumder
DHEP, TIFR

Contents

Abstract

In this report, we have described the various experiments done using scintillator and Resistive Plate Chamber (RPC). We have experimentally determined the efficiency curves of scintillators and perfomed various experiments using the scintillators like determination of Chance Coincidence Rate, speed of muon, Propagation time in cable and number of Dynodes. We have fabricated and studied the RPC Characteristics. The I-V characteristic, the efficiency curve and the TDC spectrum for RPC have been determined using scintillator paddle as trigger system. The resistivity measurement of glass and calibration of Mass Flow Controller is also described.

Chapter 1

Introduction

This chapter gives the basic introduction to atmospheric muons, atmospheric neutrinos and the INO Project,. The experiments described in the report are related to the Resistive Plate Chamber and Scintillator which are important part of the INO project. The section 1.1 explains the atmospheric muon which is used as a charged particle for all the experiments. The chapter 2 describes the characteristics of scintillator and experiments performed using scintillators. The Chapter 3 describes the working, fabrication and characteristics of RPC.

1.1 Atmospheric Muon

The muon is an elementary particle like electron. Muon is a fermion and belongs to lepton family. The charge of muon is -1 e and the mass is 105.65 MeV/c^2.

The muons are continuosly produced in the atmosphere due to the interaction of cosmic rays with air molecules. The cosmic rays mostly high energy protons when interact with the nitrogen and oxygen molecules result into the production of measons mostly pi measons which are also called pions. The pion decays into muon and neutrino.

$$\pi^- \rightarrow \mu^- + \overline{\nu}_\mu \tag{1.1}$$

$$\pi^+ \rightarrow \mu^+ + \nu_\mu \tag{1.2}$$

The muon decays further into electron and neutrinos with a life time of 2.2

μs.

$$\mu^+ \rightarrow e^+ + \overline{\nu}_\mu + \nu_e \tag{1.3}$$
$$\mu^- \rightarrow e^- + \nu_\mu + \overline{\nu}_e \tag{1.4}$$

The high energy muons are able to reach the surface of the Earth before they decay into the electrons. The muon flux at the sea level is about 1 muon per cm^2 per minute. The muon loose their energy at fairly constant rate of 2 MeV per g/cm^2. The vertical depth of atmosphere is about 1000 g/cm^2. Thus, muons loose about 2 GeV energy and reach the sea level with the average energy of 4 GeV.

1.2 Atmospheric Neutrino

The neutrino is an elementary particle and lies under the category of Leptons. The neutrino can be found in three flavours which are electron, muon and tau neutrino. The neutrino is nearly massless and neutral partical. The recent studies have shown that the neutrino has very small mass which is less than 1 eV/c^2. The neutrino is also suspected to be able to undergo flavour exchange which is called neutrino oscillation. The current neutrino observatories are trying to find out the mass hierarchy of neutrino and the oscillation parameters.

The atmospheric neutrinos are produced in the interaction of cosmic rays with atmospheric molecules. We can see from Equations (1.1) and (1.3) that neutrinos are produces in chain reaction of the pion. The ratio of muon of neutrino and antineutrino to electron neutrino and antineutrino is about 2. The muon which is able to reach the surface of the Earth is accompanied by just 1 muon neutrino or antineutrino, thus the ratio of muon to electron neutrino is more than 2 for neutrino with high energy.

1.3 INO Project

INO is a multi-institutional Mega science project which aims at building a world class underground neutrino observatory at Pottipuram in Bodhi West hills of Theni District of Tamilnadu. The proposed facility will be having 50 kton of magnetized Iron CALorimeter (ICAL) which will be stacked as plates with Resistive Plate Chambers (RPC) placed between them. Total

28800 1 m $\times$ 1 m RPC will be fabricated for this facility. ICAL will do a high precision measurement of neutrino oscillation parameter and determine neutrino mass hierarchy.

The ICAL detector will detect the atmospheric neutrinos. When the neutrino interacts with protons or neutrons of matter it produces muon which can be detected by the Resistive Plate Chamber detectors used in ICAL. The atmospheric muon background is very high at the surface, thus the detection of neutrino can be done only under the surface of Earth or high density rocks which absorb all the background radiation.

The neutrino interaction cross section is very less, it can go through 50 light years of Lead without interacting. The low cross section requires a high density material as passive region in the detector to get at least few counts per year. The magnetised Iron Calorimeter will serve two perpose, one it will provide high density material for neutrino interaction and other, it will create very high magnetic field (about 1.3 Tesla) which will be used to distinguish muon and anti muon. Thus, the muon neutrino and antineutrino can be distinguished by the ICAL.

In this report, we have expained the scintillator and RPC. The scintillators were used as trigger for the RPC. The RPC facbrication and determination of characteristic curves is explained in the Chapter 3.

Chapter 2

Experiments with the Scintillator Detector

2.1 Introduction

The scintillator detectors which we are using are consisting of plastic scintillator, a light guide and photomultiplier tube (PMT). The plastic scintillator produces photons when a muon passes through it, the photons are guided towards the PMT by the light guide. The PMT collects the photons and produces electrons which are multiplied inside PMT. The output of PMT goes to the discriminator which selects the pulses with voltage peak greater than a discriminator threshold. The discriminator produces output in the form of the square pulse which is then counted by a scalar.

The scintillator should produce the photons when a charged particle passes through it. The scintillator should have following properties:

- High light-yield - the conversion of kinetic energy of the particle to light photons should be efficient.
- Linearity - the light emission should be linearly proportional to the energy deposited by the particle.
- Transparent - the scintillator material should be transparent to its own emission.
- Short Decay Time - the decay time should be short for a faster signal pulse.

- Refractive index - the refractive index of scintillator should be close to the refractive index of glass (1.5) which make the coupling of scintillator with PMT easier.

There are two types of scintillators: inorganic scintillator and organic scintillators. The inorganic scintillator has high light yield and better linearity but they have poor time response. The organic scintillator has a faster response but relatively lower yield. We are using plastic scintillator which is an organic scintillator.

2.1.1 Plastic Scintillator

The plastic scintillator is an organic scintillator in which the photons are produced by the transitions in the energy levels of a molecule. When an energetic particle enters the scintillator, it loses some part of its energy to the molecules of the medium. The molecules absorb the kinetic energy of the particle and go to the excited states. The higher excited states are very unstable and decay through a non-radiative transition to lower excited states. The lower excited states decay directly to the ground state resulting in the emission of a photon and this phenomenon is called fluorescence. The energies of lower excited states are lower than that of higher states thus the emitted photon are less energetic than the photons required for absorption. Thus, these photons are not absorbed back and the scintillator material becomes transparent for them.

The lifetime of the excited state is very less which results in the sharp signals. The emitted photons have the wavelength in the blue or UV region. The scintillator is covered with the Tyvec paper which reflects the emitted light back into the medium. Then, the scintillator is wrapped in the Tedlar paper which prevents are ambient light from entering into the scintillator. The properties of the scintillator used are given in Table 2.1.

2.1.2 Photomultiplier Tube (PMT)

A photomultiplier tube or PMT receives photons and convert them into electrons which are then multiplied to get a signal pulse. The PMT is a vacuum tube consisting of photocathode, focusing electrode, dynodes, and anode.

Table 2.1: Scintillator detector specifications.

Manufacturer	Bicron
Type	Plastic
Model No	BC-408
Light output, % Anthracene	64
Wavelength of max emission in (nm)	425
Rise Time	0.9 ns
Decay Time	2.1 ns
Pulse Width, FWHM	$\approx$ 2.5 ns
Light Attenuation Length	210 cm
No. of H Atoms per $cm^3, (\times 10^{22})$	5.23
No. of C Atoms per $cm^3, (\times 10^{22})$	4.74
Ratio H:C Atoms	1.104
No. of Electrons per $cm^3, (\times 10^{23})$	3.37
Principal uses/applications	TOF counters, large area

The photocathode receives the photons and produces photoelectrons through the process of the photoelectric effect. The photon strikes the outer surface of the photocathode and the transfers its energy to the electron which diffuses toward the surface of the photocathode. The electrons with sufficient energy are able to get out of the surface of the photocathode and enter into the vacuum. High voltage is applied to the focusing electrode which creates an electric field in which electrons are accelerated towards the first dynode. The Focussing electrode decides the collection efficiency of the first dynode.

The electron striking the surface of dynode result into the emission of secondary electrons. A high voltage is applied between the successive dynodes, thus the secondary electrons emitted from the first dynode are accelerated towards the second dynode. The electrons moving towards the second dynode gains enough energy to produce more secondary electrons. The number of electrons increases as they pass through the each dynode stage. The number of secondary electrons produced by a single electron is called secondary electron ratio which depends upon the energy of electrons which in turn is dependent on the high voltage applied between two successive dynodes. Consider g be the secondary electron ratio, then after the n dynodes a single electron will be multiplied to g^n. The electrons emitted by the n^{th} dynode are collected by the anode which gives the output to the external

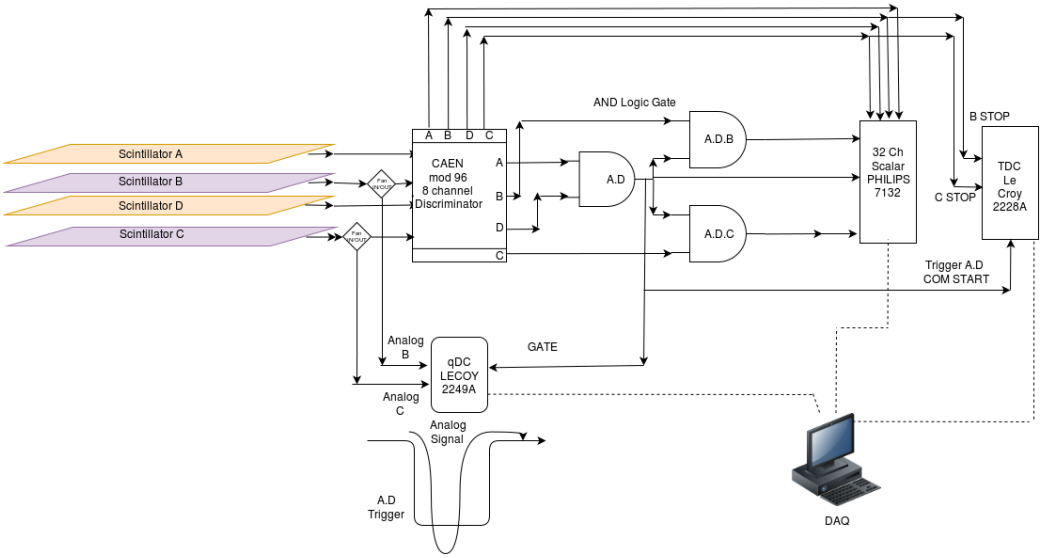

Figure 2.1: Circuit for efficiency of Scientillators

cable. The external cable takes the output of the discriminator. The total charge collected depends upon the photon to electron conversion efficiency, the collection of photoelectrons, the secondary electron ratio and the number of dynode stages.

2.2 Efficiency of the Scintillator Paddle

The efficiency of the scintillator paddle depends on the voltage applied to the PMT. We want the scintillator to operate at the voltage where efficiency is highest. But the application of the high voltage results in increase in the noise rate and also the decrease in the life of scintillator. Thus, we want to find the optimum operating voltage for scintillator where the efficiency is highest and the noise rate is as low as possible.

To find out the operating voltage, we measured the efficiency of scintillator paddle at various voltages and plot that as a function of voltage. We had four paddles named as A, B, C and D. We placed the paddles one over the other so that the maximum number of muon pass through all four of them. The order of paddles from top to bottom was A, B, D and C. A constant voltage of 1600 V was applied to the paddles A and D and the voltage applied to paddles B and C was varied from 1100 V to 1950 V. We took the

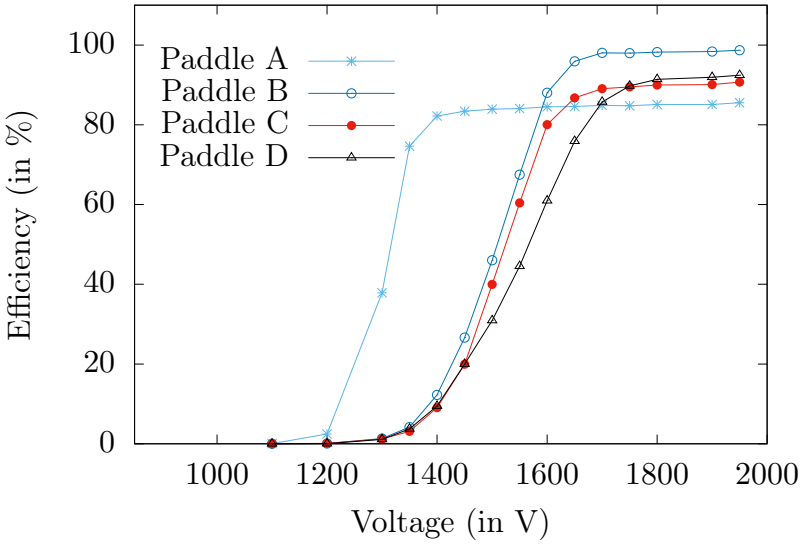

Figure 2.2: Efficiency curve for All the paddles

two-fold coincidence AD of paddle A and D which was used as a trigger. The three-fold coincidence ADB and ADC were also taken for paddle B and C respectively. All four individual counts, two-fold trigger (AD) and three-fold coincidence ADB and ADC were connected to the scalar which recorded the total counts for approximately 1 hours for each voltage applied to paddle B and C. The efficiency can be calculated as

$$\text{Efficiency} = \frac{\text{Three fold Rate}}{\text{Two fold Rate}}, \tag{2.1}$$

$$\eta_B = \frac{R_{ADB}}{R_{AD}}, \tag{2.2}$$

$$\eta_C = \frac{R_{ADC}}{R_{AD}}, \tag{2.3}$$

where, η_B and η_C are the efficiencies of paddle B and C respectively, R_{ADB}, R_{ADC} and R_{AD} are rates of ADB, ADC and AD respectively.

To find the efficiency of paddles A and D, we replaced the paddle A by paddle B and paddle D by paddle C. Now, the constant voltage 1750 V was applied across paddles B and C whereas the variable voltage from 1100 V to 1950 V was applied across the paddles A and D. We calculated the efficiency for paddles A and D also using the above formula (2.1).

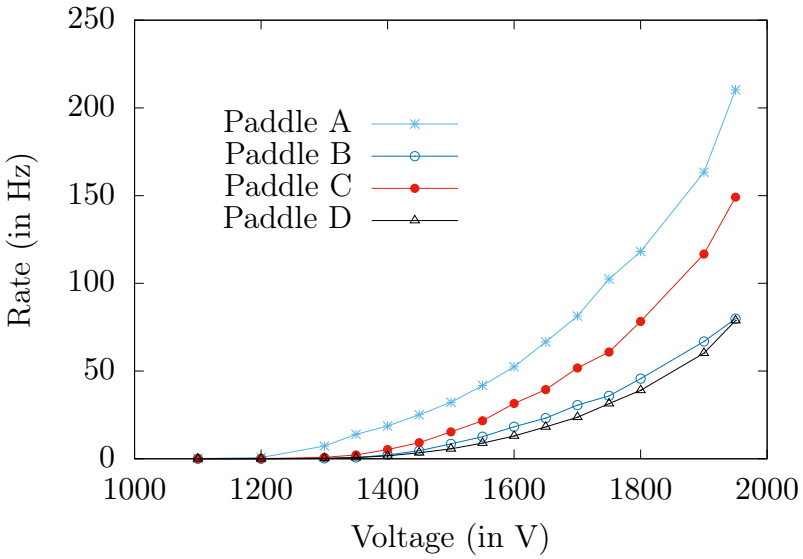

Figure 2.3: Rates of paddle with voltage variation

The efficiencies for different paddles were plotted as a function of voltage in Figure 2.2. We can see that the efficiency become indepedent of voltage at high voltages, this region of constant efficiency is called Plateau region. The scintillator should be operated in the plateau region, the starting voltage of plateau region have lowest noise. The count rates of individual paddles were also plotted as function of voltage in Figure 2.3. We can see that the count rates increases exponentially with the applied voltage. The noise rate also increases exponentially, thus, we should not applied too high voltage in the Plateau region.

2.3 Chance Coincidence

The Scintillator paddle produces a signal whenever a muon is passed through the paddle but it also produces additional signals due to noise. We place one paddle over another and try to look for those signals which appear at the same time in both paddles. These signals correspond to the passing of muon and used as a trigger system. Since, the noise signal is also present, so there is always a finite probability that two random signals from two different paddles just appears at the same time which will generate a false trigger

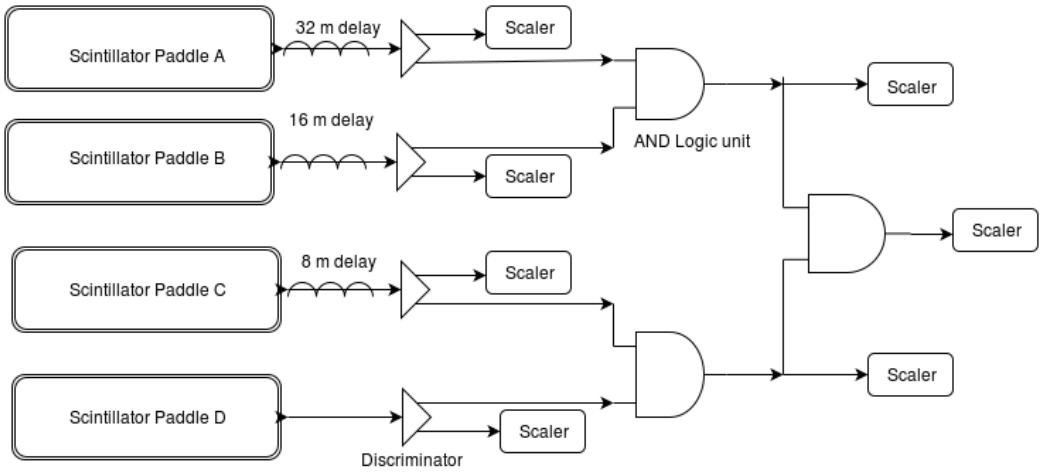

Figure 2.4: Circuit for Chance Coincidence

even in the absence of passing of muon. We do not want these false trigger signals because they produce an error in the counts of muons. We are doing this experiment to ensure that this chance coincidence rate is negligible.

To find out only chance coincidence, we need to remove all the correlated coincidences. We need to ensure that no coincidence is produced due to the passage of muon, i.e. no muon should pass through the two paddles. We placed all the four paddles A, B, C and D side by side on the horizontal surface, this will ensure that the muon moving downward will pass through only one paddle. The coincidence can occur due to the electronic correlation also, so we introduced the time delay in the signal by adding additional cable. We added 32 m, 16 m and 8 m additional cables to paddle A, B, and C respectively.

The chance coincidence is a random phenomenon and the rate for n-fold chance coincidence can be calculated as

$$R_{12\ldots n} = n \prod_{i=1}^{n} R_i (\Delta T)^{n-1}, \tag{2.4}$$

where $R_{12\ldots n}$ is n-fold chance coincidence rate, R_i is the rate of i^{th} signal, ΔT is the pulse width which is assumed to be same for all the signal. The rate

Table 2.2: Two-fold (AB and CD) and four-fold (ABCD) chance coincidence rates

Paddle	**Total Count**	**Observed Rate**	**Calculated Rate**
A	8771625	104.4241	
B	3176286	37.81292	
C	2775091	33.03679	
D	1154338	13.74211	
AB	28	0.00033333	0.0001579433
CD	33	0.00039286	1.82E-05
ABCD	0	0	5.74E-17

for two-fold, three-fold and four-fold coincidences can be calculated as

$$R_{12} = 2R_1R_2\Delta T \quad (2.5)$$

$$R_{123} = 3R_1R_2R_3(\Delta T)^2 \quad (2.6)$$

$$R_{1234} = 4R_1R_2R_3R_4(\Delta T)^3 \quad (2.7)$$

The signal from scintillator goes to the discriminator which produces a square pulse for those pulses whose peak voltage is larger than discriminator voltage. The discriminator output for two different paddles goes to the logic unit where we have used AND GATE which will produce a signal only when two pulses overlap. The logic unit can take total 4 input and output can be 2 fold, 3 fold or 4 fold coincidence. The complete circuit is shown in Figure 2.4 where we have taken individual counts of all the paddles, two-fold coincidences AB and CD and 4 fold coincidence ABCD.

The result for above configuration is shown in Table 2.2. To get three-fold coincidence, we turned off the input C in the logic unit and made the output as 1 fold coincidence which resulted in all four individual paddle counts, one 2 fold count AB and one 3 fold count ABD. The result for three-fold coincidence ABD is shown in the Table 2.3.

To find out the three-fold coincidence ABC, we turned off the input D in logic unit and made the output as 1 fold coincidence. We also introduced the cable of 8 m length to paddle C. This configuration resulted in 4 individual paddle counts, one two fold coincidence AB and one three-fold coincidence ABC. The result for the three-fold coincidence ABC is shown in the Table 2.4.

Table 2.3: Two-fold (AB) and Three-fold (ABD) chance coincidence rates

Paddle	**Total Count**	**Observed Rate**	**Calculated Rate**
A	9629880	106.99867	
B	3469803	38.553367	
C	2988976	33.210844	
D	1233650	13.707222	
AB	23	0.000255556	0.0001650064
ABD	0	0	6.79E-11

Table 2.4: Two-fold (AB) and Three-fold (ABC) chance coincidence rates

Paddle	**Total Count**	**Observed Rate**	**Calculated Rate**
A	8534691	106.550449	
B	3063700	38.2484394	
C	2649540	33.077902	
D	1097770	13.704993	
AB	26	0.000324594	0.0001630155
ABC	3	3.75E-05	1.62E-10

2.4 Speed of Muon

The muons are produced in the atmosphere at very high energies and thus they travel at very high speed. The speed of muon can be measured using the scintillator paddles. When one scintillator is placed over other and the coincidence between their signals corresponds to the passing of muon through both the scintillator paddles. The two-fold coincidence between two scintillators in the above manner can be used as muon detector. We used total four paddles, two paddles were used as a trigger which started the TDC counter and other two paddles were used as stop trigger. The four paddles were named as A, B, C and D. The paddle A and B for stop trigger were placed at the bottom and the paddle C and D for start trigger were placed at the various heights. All the paddle should be aligned properly to receive the maximum number of counts.

The muons produced in the atmosphere hit the surface at different angles which follow the cosine distribution. Consider θ be the angle between the direction of muon and the vertical axis, θ can also be called zenith angle. The number of muons with zenith angle θ is proportional to $\sin\theta\cos^2\theta$. Thus,

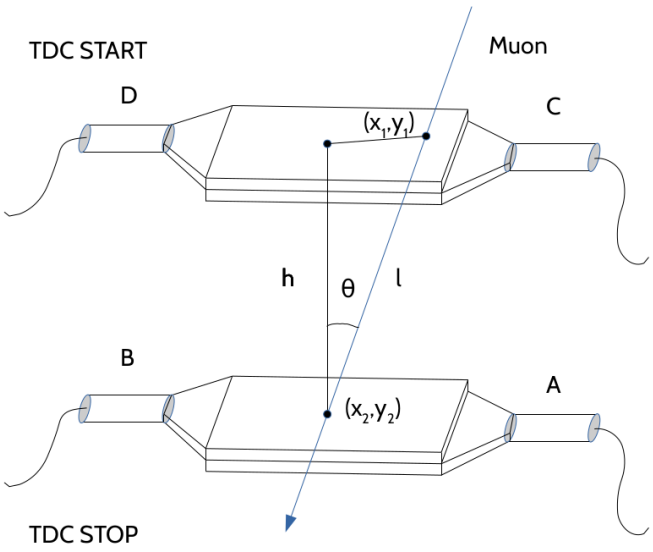

Figure 2.5: Setup for measuring speed of muon

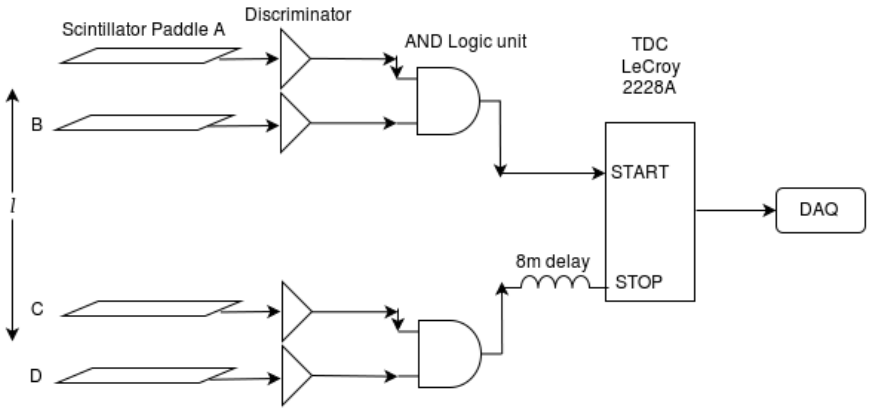

Figure 2.6: Circuit for measuring speed of muon

the number of muons will be highest along the vertical direction with $\theta = 0^\circ$ and least along the horizontal direction where $\theta = 90^\circ$. The muon passing through the scintillator setup will actually be traveling through a path which is more than h, the difference of height between the top and bottom paddles. The actual path traveled by the muon will be $h/\cos\theta$ which will be equal to h, only in the case of $\theta = 0^\circ$.

We have calculated the average path traveled by muon by considering one random point on the top scintillator paddles (C and D) and another random point on the bottom ones (A and B). The dimensions of paddle A, B and C were 40 cm $\times$ 20 cm and the paddle D was smaller with dimension 28 cm $\times$ 15 cm . We considered the dimension of D in the top paddles for calculation because this is the common area between paddle C and D which give rise to coincidence signals. We considered the first random point (x_1, y_1) on the paddle C and D and the second random point (x_2, y_2) on the paddle A and B where:

$$x_1 = l_{CD} \times \text{random-number}, \tag{2.8}$$

$$y_1 = w_{CD} \times \text{random-number}, \tag{2.9}$$

$$x_2 = l_{AB} \times \text{random-number}, \tag{2.10}$$

$$y_2 = w_{AB} \times \text{random-number}, \tag{2.11}$$

where l_{CD} is the length of the paddle D, w_{CD} is the width of the paddle D, l_{AB} is the length of the paddle A, w_{AB} is the width of the paddle A and random number can vary between 0 and 1. The distance l between these two random points can be calculated as :

$$l = \sqrt{(x_1 - x_2)^2 + (y_1 - y_2)^2 + h^2}. \tag{2.12}$$

The muon flux follows the cosine distribution so we need to do the averaging of l over cosine distribution, i.e.

$$\bar{l} = \frac{\sum \sin\theta \cos^2\theta \; l}{\sum \sin\theta \cos^2\theta}, \tag{2.13}$$

where, the summation is done over the number of iteration we are performing. The error in the calculated average path $\bar{l}$ will decrease with the increasing number of iterations. We performed 100000 iterations.

The TDC counter gives the time delay between the start and stop trigger. The time delay corresponds to the time required by muon to travel from top

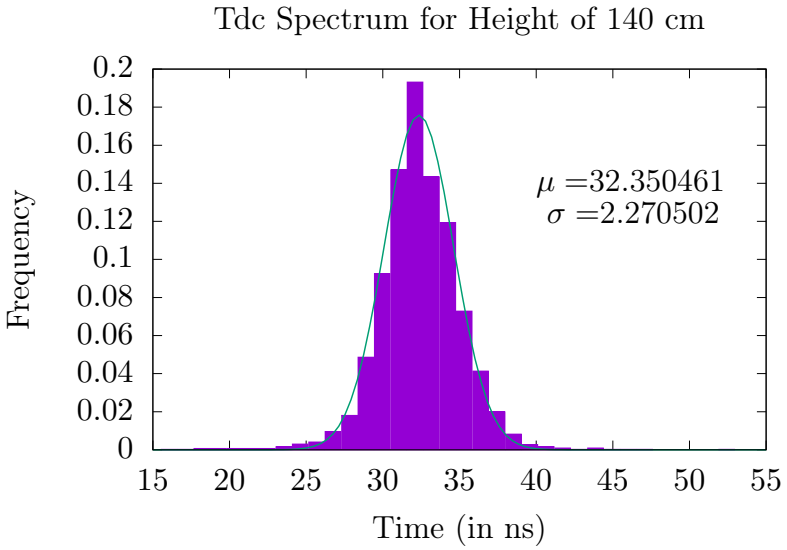

Figure 2.7: TDC Spectrum fitted with gaussian distribution

paddles to bottom paddles and the delay in the electronic circuit. The TDC distribution for the muon follows the gaussian distribution which is shown the Figure 2.5. We fitted the gaussian distribution to find out the mean of the measured TDC distribution. This mean will be used as the time delay for finding the velocity of the muon. We measured the time delay for various heights, i.e. 4.5 cm, 28 cm, 86 cm, 111.5 cm, 140 cm and 201 cm.

The graph is plotted between the time delay on the y-axis and the height on the x-axis. The linear fit will give us the slope and intercept. The equation for linear fit will be :

$$y = mx + c, \tag{2.14}$$

where, m is the slope. The speed of the muon can be calculated from the slope

$$v = 1/m. \tag{2.15}$$

The obeserved speed of muon is $(2.8 \pm 0.2) \times 10^8$ m/s which is

$$v_{obs} = 0.96c \pm 0.07 \tag{2.16}$$

$$v_{data} = 0.99c \tag{2.17}$$

The error mentioned here is the linear fitting error in the graph. The standard

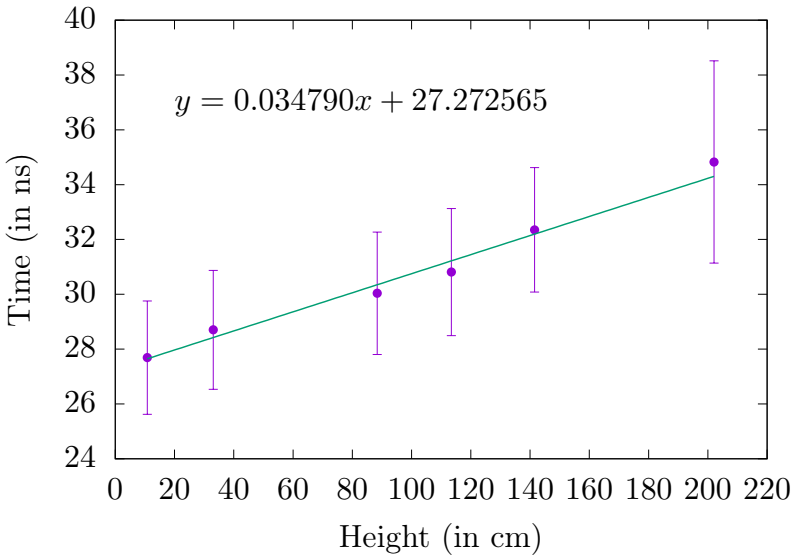

Figure 2.8: Speed of Muon

deviations obtained from the gaussian fitting are used as the weights for data points in the linear fitting, thus the gaussian spread has taken into account.

2.5 Propagation time in cable

The electronic signal travels at a finite speed in the cable. The finite speed results in the delay which increases linearly with the length of the cable. In this experiment, we measured the delay introduced due to the length of the LEMO cable. The setup for measuring delay in the cable is similar to the

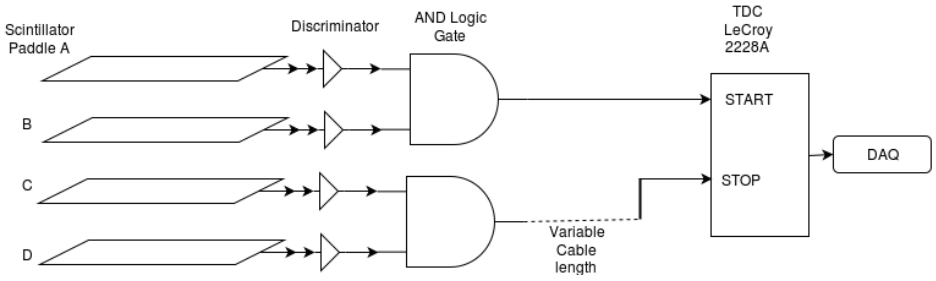

Figure 2.9: Circuit for measuring delay in LEMO cable

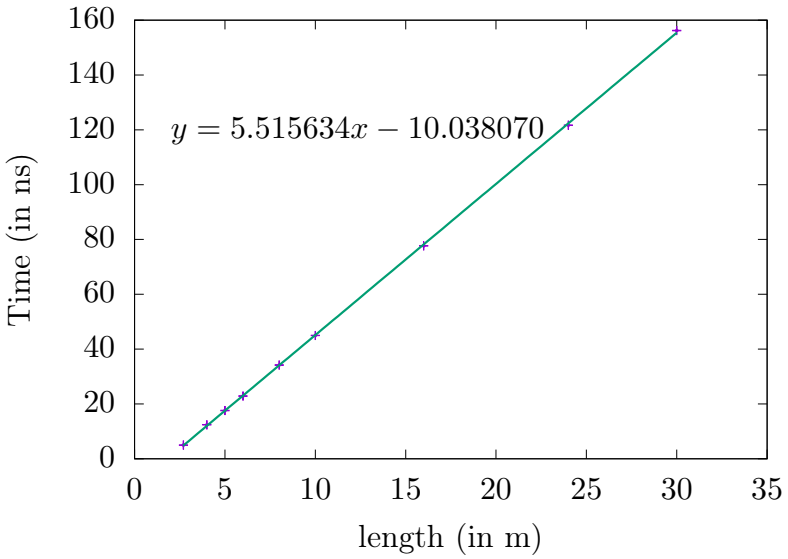

Figure 2.10: Time Delay in LEMO Cable

setup required for the measurement of the speed of the muon. But in this case, top paddles will be placed on the bottom paddles which corresponds to the case of minimum height in the previous setup.

The time delay will be present even if both TDC START and TDC STOP have same cable length because the electronic circuit always introduces the time delay. The TDC START pulse should reach the TDC earlier than TDC STOP pulse, to ensure this, we introduced extra cable to TDC STOP. This configuration corresponds to basic delay due to the circuit which we noted as the time delay in case of 0 m cable. Then, we added cable of various length to TDC STOP and measured the time delay for each added cable. The extra cable which we used for delay are 2.7 m, 4 m, 5 m, 6 m, 8 m, 10 m, 16 m, 24 m and 30 m.

The graph was plotted between time delay on the y-axis and cable length on the x-axis. The linear fitting was done where slope will give the time delay due to 1 m cable and y-intercept will give the delay due to the electronic circuit. The slope intercept form of the linear equation is

$$y = mx + c, \tag{2.18}$$

where m is slope and c is intercept.

The time delay observed in the LEMO cable is (5.52 ± 0.02) ns/m. The error mentioned here is the fitting error, the errors due to least count have been taken into account while fitting.

2.6 The number of dynode stages

The charge produced in a single pulse depends upon the various factors like the energy of muon, the no of photons produced, the photon to electrons conversion efficiency, the photoelectron collection efficiency, no of dynodes and the applied voltage to scintillator.

Consider, the secondary electron ratio is g which is the number of secondary electrons produced by a single electron when it strikes the surface of dynode. This ratio depends upon the energy of electron which in turn depends upon the accelerating potential between two successive dynodes.

$$g \propto V \tag{2.19}$$

Consider, the number of dynodes in the PMT be N then the total charge collected will be

$$Q \propto g^N, \tag{2.20}$$

where Q is total charge collected by the anode. From the above two equations (2.19) and (2.20), we can see that

$$Q \propto V^N, \tag{2.21}$$

$$Q = kV^N, \tag{2.22}$$

where k is proportionality constant. We can get the number of dynodes stage by plotting the charge Q and the applied Voltage V on logarithmic scale

$$\ln Q = N \ln V + \ln k, \tag{2.23}$$

where $\ln Q$ will be the y-axis and $\ln V$ will be the x-axis. The slope will give the number of dynodes N

$$N = \text{Slope}. \tag{2.24}$$

The charge in each pulse is measured by the ADC. We have measured the ADC distribution for various voltage from 1100 V to 1950 V for all the paddles. The QDC distribution was measured on the same setup used for efficiency measurement of paddles.

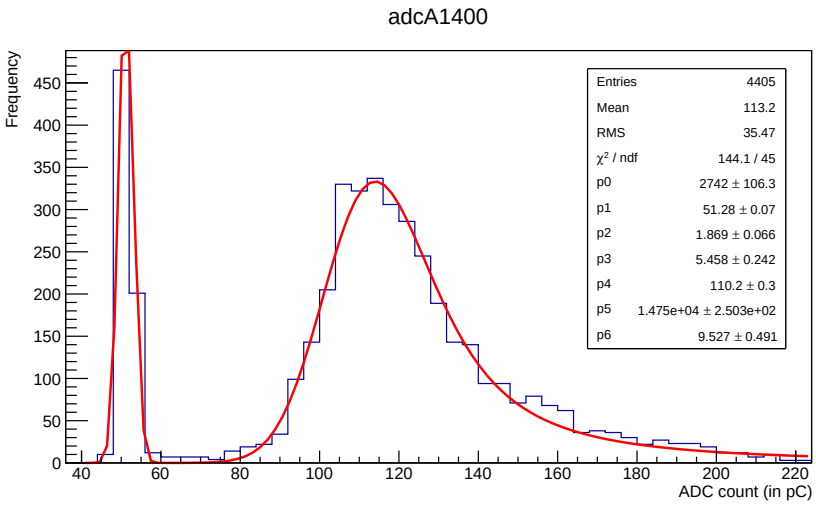

Figure 2.11: The ADC specturm for Scintillator paddle A at 1400 V

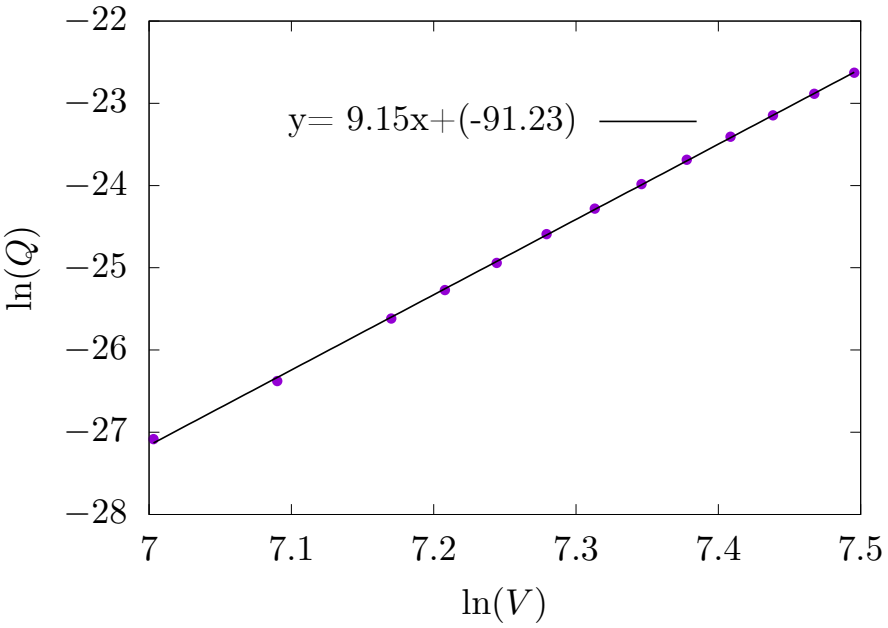

Figure 2.12: The number of diode in PMT of paddle A

The Figure (2.12) shows the ADC spectrum for Scintillator paddle A at 1400 V. The peak at left corrosponds to the padestal which follows gaussian distribution and the peak on the right is due to signal pulses which follow Landau distribution. The Figure (2.12) shows the graph between $\ln V$ and $\ln Q$ where the slope should be equal to the number of dynodes in the PMT.

$$\text{slope} = 9.15 \pm 0.04 \tag{2.25}$$

$$\text{No. of dynode} = 9 \tag{2.26}$$

Chapter 3

RPC Fabrication and Characterization

3.1 Introduction

This chapter describes the working of Resistive Plate Chamber, Gas mixture, fabrication and Characterisation of RPC. We fabricated three RPC of dimension 30 cm $\times$ 30 cm, then the I-V characteristic and Efficiency curve were determined for them. The resistivity measurement of glass and calibration of MFC was also performed as part of fabrication.

3.2 Resistive Plate Chamber

In the gas detectors, multi-wire proportional chambers were the earlier detectors. In this detector, the charged particle produces ionization and results in the electrons which are collected by anode wire. The charge produces in anode wire is proportional to the energy deposited by the charged particle. But this detector had an electric field dependent on r which lead to the poor time resolution.

This problem is not present in the Resistive Plate Chamber (RPC) which consists of two parallel plates of very high resistivity and coating of a conductive material like graphite on the surface. The electric field between parallel plates is uniform. When a charged particle enters the chamber, the particles loses its energy and ionizes the gas molecules which is called primary ionization. The primary ionization of gas molecules creates electron-ion pairs which

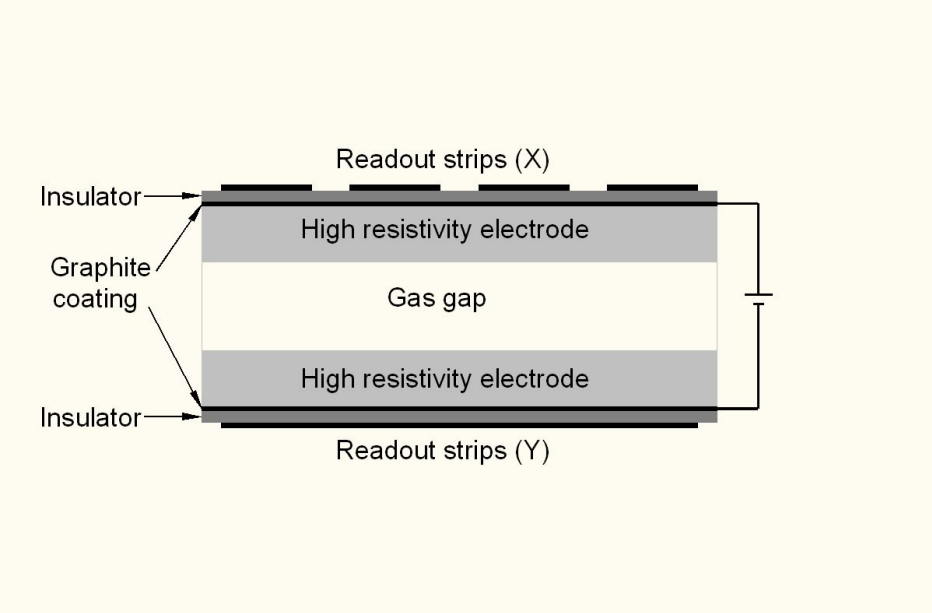

Figure 3.1: Layout of RPC

get accelerated by the high electric field between parallel plate electrodes. As the electrons get accelerated, they acquire kinetic energy and collide with other molecules of the gas which result in the ionization of the gas molecule. This is called secondary ionization which results in the avalanche.

The electrons moves towards the anode and ions moves towards cathode. The electrons have larger drift velocity and thus they reach the anode surface much faster as compared to positive ions. While going towards anode the avalanche is created and when all these negative charged ions reach anode, the decharge happens. The positive ions are slow but they also reach the cathode plate after some delay. The field in this region drops significantly and this small area of order 0.1cm^2 remain dead until the electrode gets charged up again which takes about 2 s. The other regions of detector function normally during this dead time.

The discharge happens at a very short timescale of 1 ns which is much faster than that of the cylindrical detectors (100 ns). This mode of operation is called **avalanche mode** which happens at a lower voltage. Our RPCs are operating is the avalanche mode which gives a signal of the order of few mV. Thus, we require amplifier to get sufficient voltage but avalanche mode

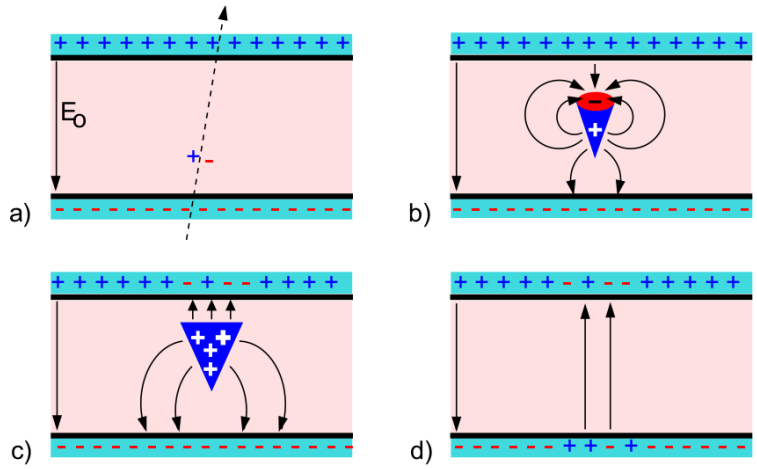

Figure 3.2: Development of Avalanche. a) Primary ionization in the path of charged particle and avalanche is started. b) The avalanche size is sufficiently large to influence the electric field in the gas gap. c) The electrons reach the anode but ions are slow. d) The ions also reach the cathode surface.

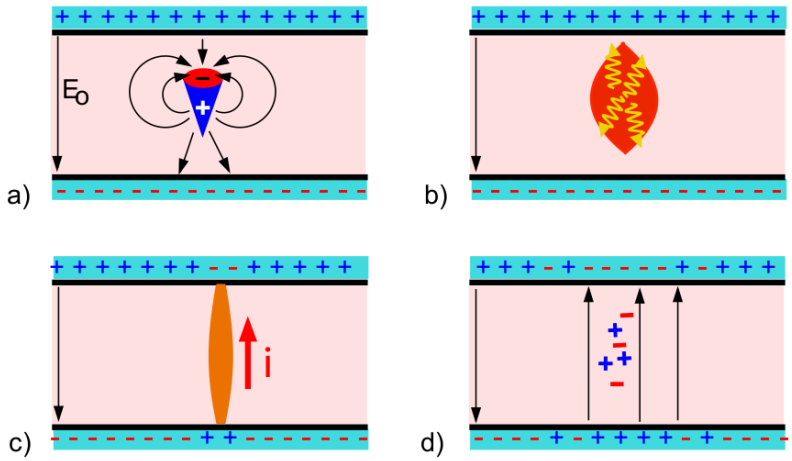

Figure 3.3: Development of Streamer. a) An avalanche is developing. b) The avalanche charges lead to a high field detoriation in the gas gap. A streamer evolves c) A weak spark may be created. The local electrode area is discharged. d) The electric field is strongly decreased around the spot of the avalanche.

provides longer lifetime of RPC.

If the voltage across the parallel plates is very high than the electron-ion pairs will keep on growing and the steamer of plasma will be formed between the electrodes. Thus, the electrode will get discharged through this streamer. The electric field drop significantly as compared to the avalache mode. This mode of operation is called **streamer mode**. The streamer mode gives very high voltage signal of the order of 100-200 mV and does not require amplifier. The lifetime of RPC is lesser in this mode as compared to the avalanche mode.

The plates can be made up of glass or bakelite. The RPCs are very easy to make and are very economical. The main features of the RPC are :

- Good timing resolution.
- Large signal output
- Excellent position resolution
- Cost effective

3.3 Gas Mixture

The component of the gas Mixture is decided by the several factors such as low working voltage, high gain, good proportionality and high rate capability. Consider the number of primary electrons produced be n_0, then the number of electrons reaching the anode will be given by

$$n = n_0 e^{\eta x}, \tag{3.1}$$

$$\eta = \alpha - \beta, \tag{3.2}$$

where, α is the first Townsend coefficient which depends upon the number of ionization per unit length, β is the attachment coefficient which depends upon the number of electrons captured per unit length.

For low working voltage, noble gasses are selected which have low ionization potential. For low ionization potential, we are using Freon (R134a) which decides the first Townsend coefficient.

When electron-ion pairs are formed, they have a tendency to recombine. The recombination of electron-ion pair results in the emission of ultraviolet photons which have enough energy to break electron-ion pair at some other

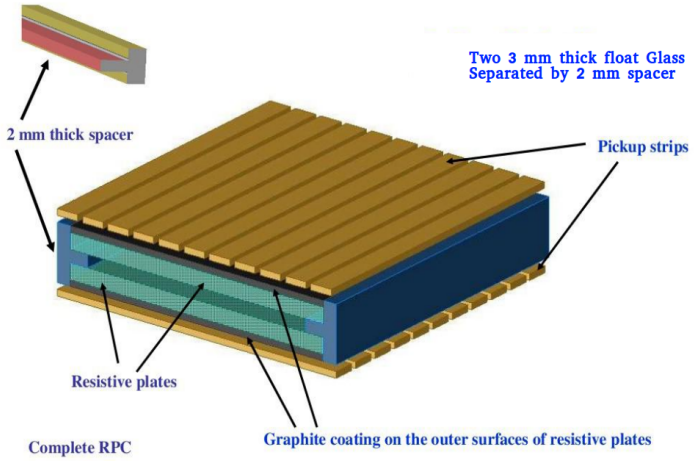

Figure 3.4: Structure of RPC

place in the chamber. If this happens then we will loose the spatial resolution and the avalanche will take place in the entire chamber. A polyatomic gas is used to absorb ultraviolet photons. Usually, a hydrocarbon gas is used as the polyatomic gas. In our case, we are using Isobutane. This photon absorber gas is also called quenching gas because it limits the avalanche to a local region.

An electronegative gas is required to absorb the excess of electrons. The electronegative gas has high electron affinity. In our case, we are using SF_6 for absorbing excess electrons.

The proportion of Freon, Isobutane and SF_6 gasses in the gas mix is 95.15 : 4.51 : 0.34 respectively.

3.4 Stucture of RPC

- The RPC consist of two parallel resistive plates which can be made up of glass or Bakelite. We are using glass plates of thickness 3 mm whose resistivity lies in the range of $10^{10} - 10^{12}$ Ωcm .

- The glass plates are coated with a resistive material which should have the resistivity of the order of 1 $M\Omega/\square$. If the resitivity is less than this the signal induction in pickup strips will be difficult due to faraday cage effect.

- The glass plates are separated by polycarbonate button spacer with a thickness of 2 mm and resistivity of 10^{13} Ωcm.
- The T-shaped edge spacer is used to seal the chamber from the sides and the corner spacer has a gas nozzle for inlet and outlet.
- The chamber is filled with a gas mixture of SF_6, isobutane and R134a (Freon) in the ratio 0.34 : 4.51 : 95.15 respectively.
- The pickup panel is composed of 5 mm thick plastic honeycomb with 2.8 cm wide pickup strip on one side and 50 μm thick aluminum foil on the other side.
- The pickup panel and high voltage resistive coating is isolated from each other by 2 mylar sheets of thickness 100 μm.

3.5 Fabrication of RPC

3.5.1 Glass cutting

We fabricated three RPCs, each of the size 30 cm $\times$ 30 cm with the normal float glass. The glasses were cut using the diamond cutter, the isosceles triangle with angle 45° and sides 2 cm were cut and removed from the corners. Total seven glass were cut in above manner (one spare). Each RPC requires 2 glasses so 6 glasses were used to make 3 RPC.

3.5.2 Glass Cleaning

All the glasses first cleaned with tissue paper (a lot of tissue paper is required for cleaning purpose) and then cleaned with distilled water. Then, the solution of labolene was prepared in distilled water which was used to clean glass plates with scrubber soaked in the labolene solution. After cleaning with the labolene solution, we washed the glass plates with distilled water by holding the glass plates over the bucket. The glass plates were then cleaned by tissue paper and left for drying in the clean place.

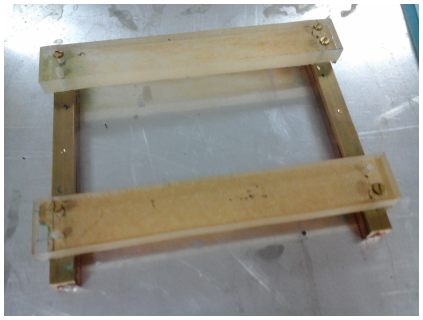

Figure 3.5: Resistance Measurement Jig

3.5.3 Resistive coating

The Thermocole was cut into pieces as per the shape of glasses and all the glasses were placed on the Thermocole pieces. The 1 cm edges of all the glasses were covered with masking tape which also fixed them on their respective Thermocole bases. The edge was covered with masking tape to protect them from graphite coating, the current may leak through the edges and may result in short circuit and also edge effect in the electric field. Now, the glasses were ready for resistive coating.

Narolac has developed a conductive paint which has been modified with additives to get resistance of 1 $M\Omega$. We dissolved the paint in thinner and used a spray gun to paint the glasses. The air pressure inside the gun results in the spray of paint. The glasses were painted with resistive coating and left for drying.

The resistance of the coating was measured using a resistance measurement jig which is a square instrument having two copper bars at one pair of opposite sides and another pair of opposite sides is free. We used a multimeter to measure the resistance of the coating surface by touching two copper bars with two leads for the multimeter.

The resistance of the glass plates was measured at the 10 different positions. The resistivity was measured again next day which was expected to increase but in our case, it was found to be similar to that of the previous day. The order of resistance was 1 $M\Omega$ and we identified the pairs having similar resistance.

3.5.4 Gluing of RPC

Once the glass were ready with 1 $M\Omega$ resistive coating on one surface of the glass, we removed the masking tape and separated them from the Thermocole pieces. We again cleaned the uncoated surface of glass with tissue paper and labolene (just small amount on tissue paper) to remove any dirt came from Thermocole.

We used the Epoxy Adhesive DP 190 Gray named as 3M Scotch-Weld which comes as the Duo-Pak cartridge of two separated thick paste which can be mixed to form glue. The paste does not dry inside the cartridge but ones it is mixed it should be used within 90 minutes otherwise it will get dried. The glue cartridge was inserted into the high-pressure gun which applies the pressure on the cartridge to get the two pastes come out. The paste was collected in a syringe (by removing the needle) and mixed by transferring into another syringe from the backside. This process was done about 10 times to mix the glue properly.

The two glass plates in RPC are separated by a polycarbonate button spacer of thickness 2 mm (the same button used in shirt) having three holes. The glue drops (one drop per spot) were applied on the uncoated side of the glass at four different spots and the four button spacers were placed on the glue. The spacers were pressed gently so that the glue comes out of the holes, now the glue drops were applied on the spacer. The another glass of this pair was placed gently on the four spacers such that the uncoated side is downward touching the spacer and get glued to the other plate through spacer. Both the plates should be properly aligned. The lead block was placed over the plates to apply the pressure and the places were left for a day for drying.

3.5.5 Gluing of Edge Spacer

The glued plates had their edge open which needed to be sealed to make a gas chamber. The edge spacer have protrudes of 2 mm and a step which leaves 1 mm space for glue. The edge space can neatly fit inside the gap in the RPC plates leaving the space for glue as you can see in Figure 3.6. The corner edge spacers are designed separately which have gas nozzle and protrudes pointing lengthwise which can fit inside the hole in the edge spacer. The gas nozzle lies inside the removed corners of plates which prevent it from damaging while transportation.

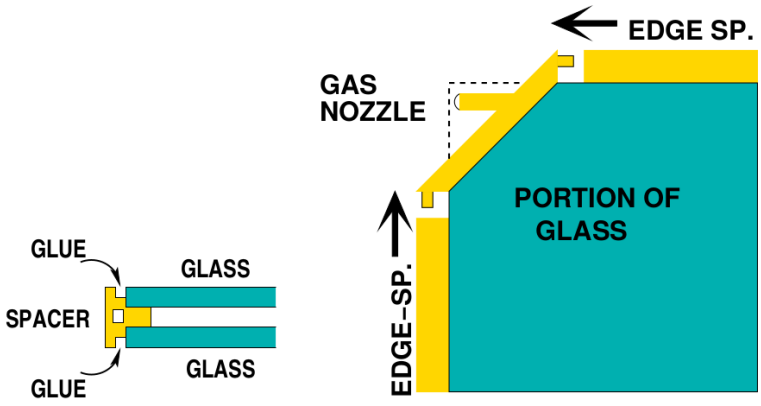

Figure 3.6: Edge spacer and corner edge spacer

Figure 3.7: RPC after applying glue to the Edge Spacer

The edge spacer was cleaned and cut according to the length of plates and checked by placing them in the RPC. The corner edge spacer was placed such that the direction of two adjacent gas nozzle is towards one direction while that of other two opposite nozzles are towards other direction. The glue was applied through syringe on the gap at the step in the edge spacer. The glue was also applied at the joints of the edge spacer and corner edge spacer. The glue can be applied only one surface at a time and thus RPCs were left for drying for one day. Next day, the RPCs were flipped and the other surface was glued and again left for drying.

3.5.6 Leak Test

The RPCs were now ready and we needed to check for any leak. The tubes were connected to the gas nozzle such that two parallel gas nozzle will act gas inlet and other two as the gas outlet. The outlet was connected to the manometer which is a U-shaped tube with water filled in the tube. The level of water was same on both the sides when nothing was connected to the one side of the manometer (other side was open and used for filling the liquid), this level was marked on the tubes. The input of the RPC was connected to the high-pressure freon gas cylinder. The gas nozzle of the cylinder was opened slowly and pressure started building up inside the RPC. The level of manometer started going down on the side where the RPC outlet was connected. When the difference of both levels became 3 cm, we stopped the gas flow. Now, the pressure inside the RPC was 3 cm of water column.

The RPC was left with this 3 cm of the water column, as the time of day changed the ambient pressure changed which resulted in the change in height of the water column in the manometer. We noted the water column height at regular interval of time. The water setup was left for overnight and we noted the pressure next day also. After 24 hours, at the same time of the day, the pressure should be same as 3 cm of water column.

After testing with pressure, we also tested in sniffer mode where the gas flows through the RPC and detect any leak using Freon detector. Before testing with a leak detector, we punctured all the bubbles created in the dried glue in RPC because these bubbles can burst later at high pressure and result in the leak which will be difficult to repair at that time. We applied the glue again on the punctured bubbles. Then, the RPCs were tested with leak detector and no leak was found (the leak detector was detecting leak while bubbles were being punctured which ensures that leak detector was

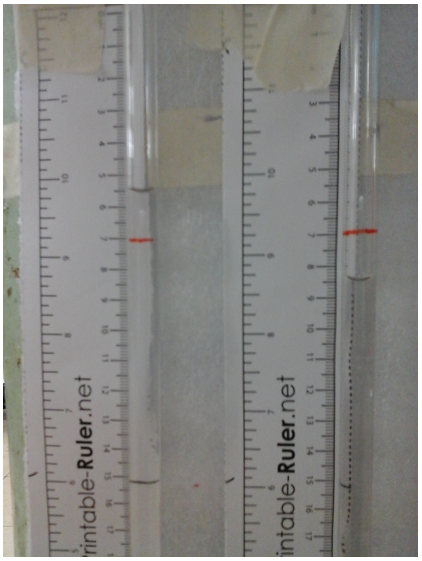

Figure 3.8: Monometer showing pressure difference of 3 cm of water column.

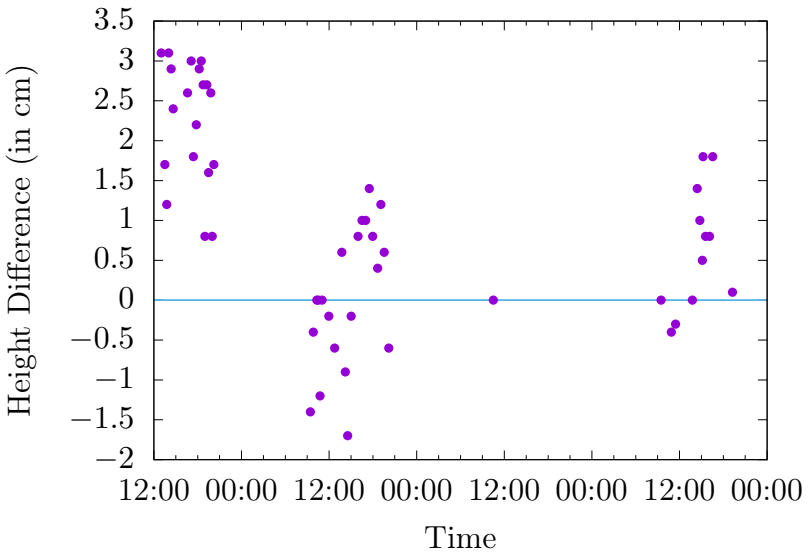

Figure 3.9: Pressure Variation in RPC C with time for three days

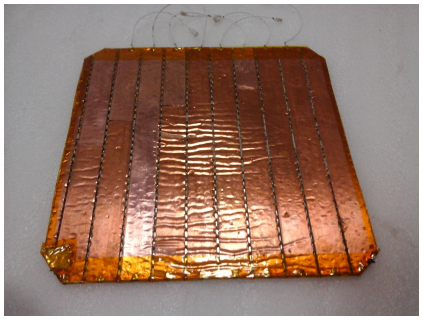

Figure 3.10: Pickup Strips

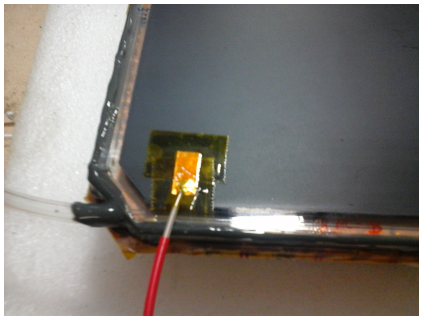

Figure 3.11: High Voltage connection through copper tape

working).

3.5.7 Pickup Panel

These RPC's were being fabricated to replaced earlier RPC's so we used the older pickup panels. The pick panel is made by gluing thin Aluminium foil on one side of honeycomb insulator and the parallel aluminum pickup strips on the other side. The thickness of pick up strip is 2.8 cm and the gap between adjacent pickup strip is 0.2 cm. The 50 Ω resistances are soldered between pickup strips and the aluminum foil. The cable for signals are soldered on another side of pick strips with live wires on pick up strips and ground wires on the Aluminium foil. The Kapton tape is stuck along edges of the pickup panel to make it insulated from the outside.

Figure 3.12: RPC after packing in pickup panels

3.5.8 High Voltage Connection

High voltage cable was soldered on the copper tape. The copper was stuck on the coated surface at the corner by leaving around 1-inch space from edges. The Kapton tape was pasted on top of the copper tape to provide strength. The other high voltage wire was also stuck on the other side of the RPC at the same place.

3.5.9 Packing of RPC

The pickup strips should be placed on RPC in a transverse direction to another pickup strips. The insulation is required between high voltage electrode (coated surface) and the pickup strips. The insulation is provided by using mylar sheet of thickness 50 μm. Two mylar sheets are placed between pickup strip and high voltage electrode. We stuck the both mylar sheets using Kapton tape on the side of the pickup panel where pickup strips are present.

The pickup panels were placed on the RPC such that the pickup strips are facing the high voltage coated surface with two mylar sheets between them. Both the strips should be perpendicular in the direction so that they can act as x and y-axis for determining the position of the muon hit. The copper tape was used to pack the RPCs, this will make the connectivity of both aluminum foils for making ground as well as will provide strength for packing. The copper tapes were cut as long pieces of about 10 cm in length and their central portion was wrapped with Kapton tape to avoid contact to pick up strips or signal wires. Now, the copper tapes were stuck at three positions on one edge of the RPC, so total 12 pieces of copper tape were used

Figure 3.13: The copper tape electrode on the surface of glass.

to pack one RPC. The Kapton tape was stuck on top of the copper tape to provide additional support. The RPCs were given the name as A, B, and C.

3.6 Resistivity of Glass

While making the RPCs, we also measured the resistivity of Hard glass as well as normal glass. The glass piece of size 2.7 cm $\times$ 2.2 cm and thickness 2 mm is used as a sample. The high voltage cable wires were soldered on the two copper tape pieces of the same size as of glass. These copper tapes were stuck to the glass, positive terminal on one surface and negative on the other surface.

The high voltage DC power supply was connected to the cable. The voltage was varied from 0 V to 3700 V for Hard glass and 0 V to 4400 V for Normal Float Glass. At very high voltage the sparking started due to edge effect, at that point, we stopped. We noted the current at each voltage after waiting some time for the current to become stable. The graph was plotted between Voltage and Current as shown in Figure 3.14.

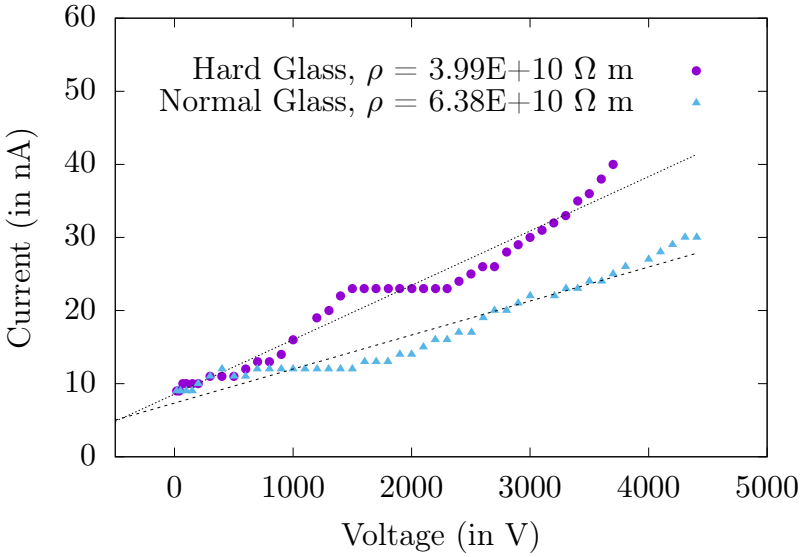

Figure 3.14: Resistivity of Hard Glass and Normal Glass

3.7 Calibration of Mass Flow Controller

The rate of gas flow is controlled by the Mass Flow Controller (MFC). It measures the amount of gas flow in standard cubic centimeter per minute (SCCM). The MFC should be calibrated for our requirement of 95.2 % of R134a, 4.5 % of Isobutane and 0.3 % of SF_6. The measurement shown on the screen of MFC may be different from the actual flow, thus we need to do the calibration of MFC.

In calibration, we will set flow at some rate say 2 SCCM and will measured the rate of flow of gas. We noted the time required to get the 10 cc volume of gas. The volume of the gas flowing was measured using test tube which was filled with water and was inverted inside the water. One end of a rubber tube was connected to the outlet of the MFC and other was inserted from below into the inverted water filled testtube. As the gas flowen into the tube, it displaced the water and got collected at the top of inverted tube. We noted the volume of the gas collected and time taken. The testtube is graduated in the unit of cubic cm, thus we get the rate as cubic cm per minute.

We measured the rate of flow for various set values on MFC. We fitted the graph and found a relationship between the set flow and the observed flow. The graphs are shown in Figures 3.15,3.17 and 3.16.

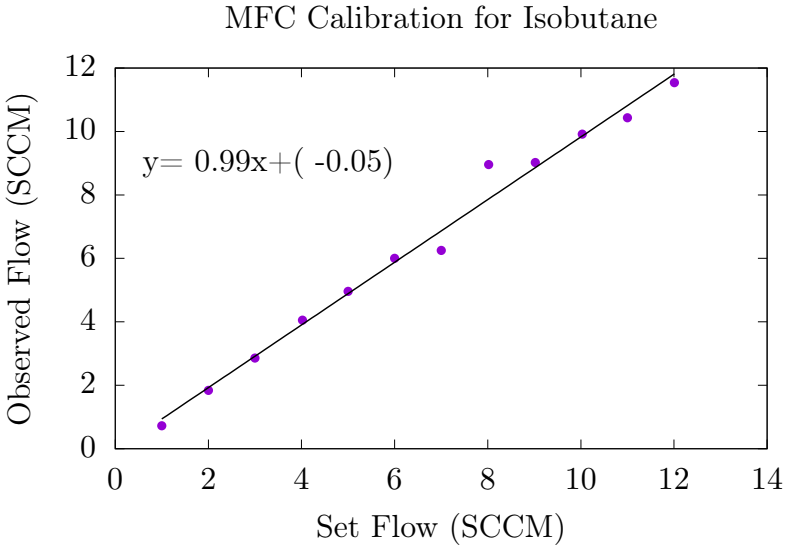

Figure 3.15: MFC Calibration for Isobutane

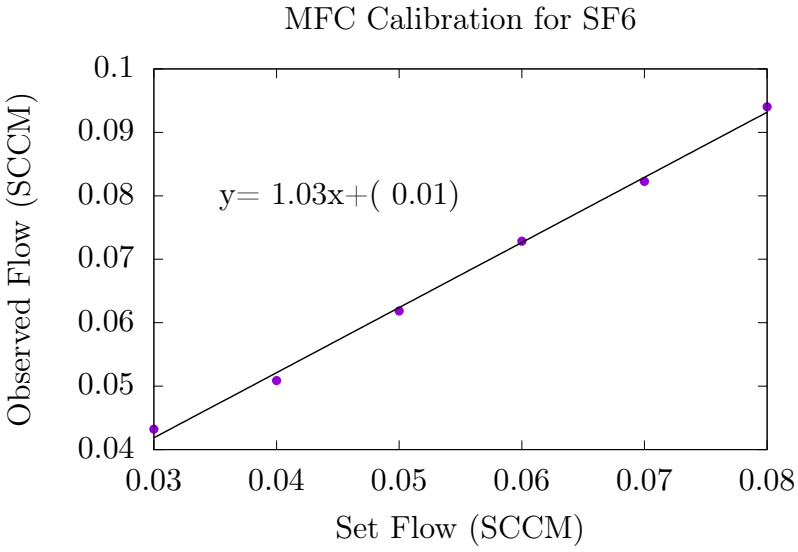

Figure 3.16: MFC Calibration for SF6

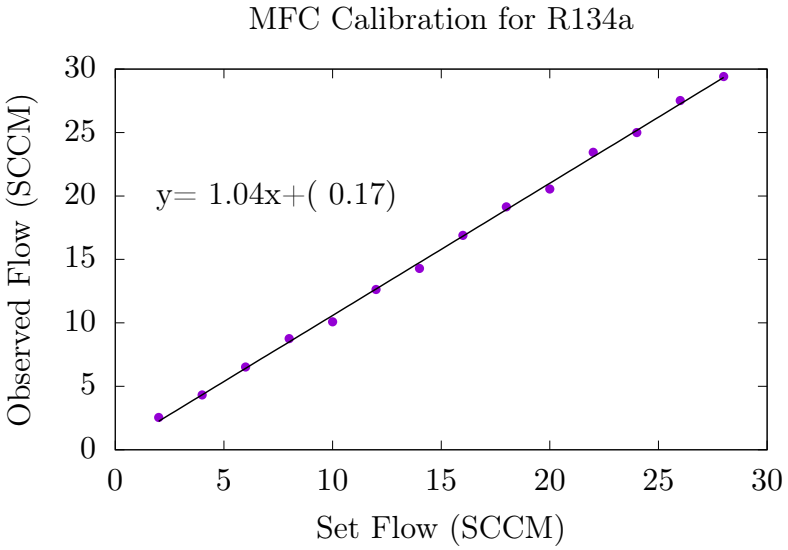

Figure 3.17: MFC Calibration for R134a

3.8 Characterisation of RPC

3.8.1 I-V characteristics of RPC

We apply positive DC high voltage to one side of the RPC and negative DC high voltage to another side of the RPC. The difference of the two voltage is the actual voltage which results in the electric field between plates. We applied the variable voltage in the region 0 V to 6000 V on both positive as well as negative side, so the total voltage across the RPC varied from 0 V to 12000 V. The current for each voltage was measured for after waiting for some time which allows the value to become stable. The I-V characteristic graphs are shown for RPC A, RPC B and RPC C in Figures 3.18, 3.19 and 3.20 respectively.

3.8.2 Efficiency

The DC voltage powers supplies were already connected during the I-V characteristic measurements. For measuring the efficiency of RPC, we used finger paddle scintillators which had a width of 3 cm. We used three finger paddles which were aligned with the third strip from the left of the top panel. The

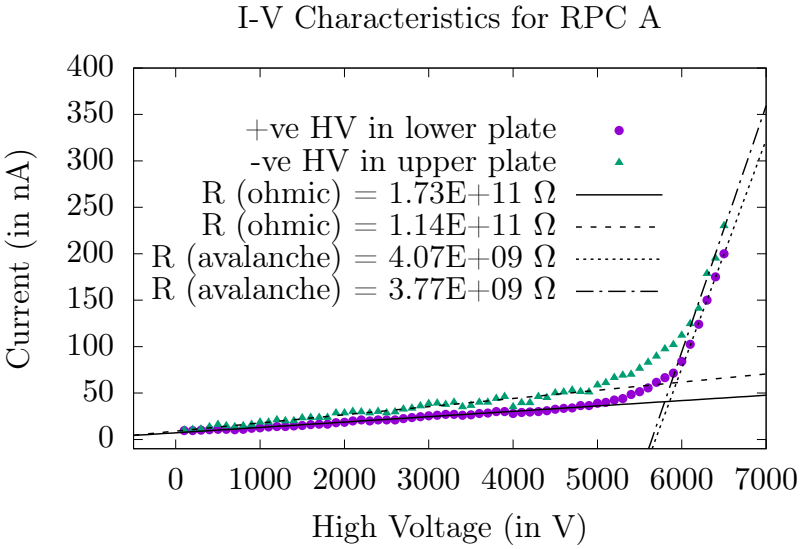

Figure 3.18: I-V Characteristics of RPC A

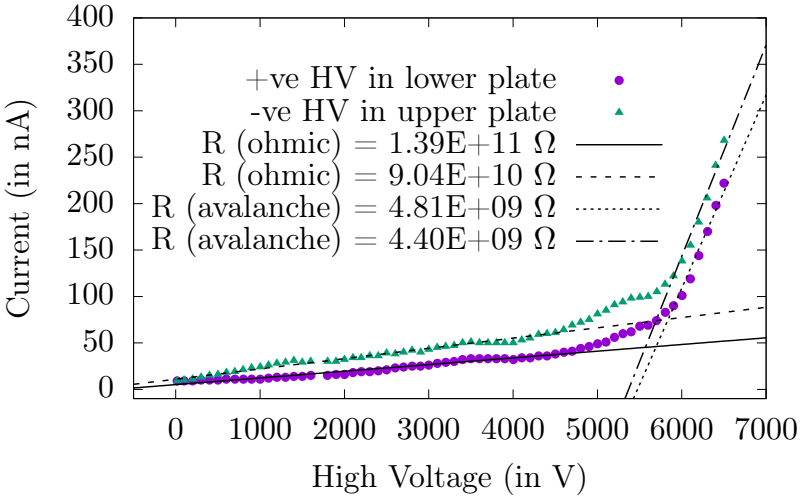

Figure 3.19: I-V Characteristics of RPC B

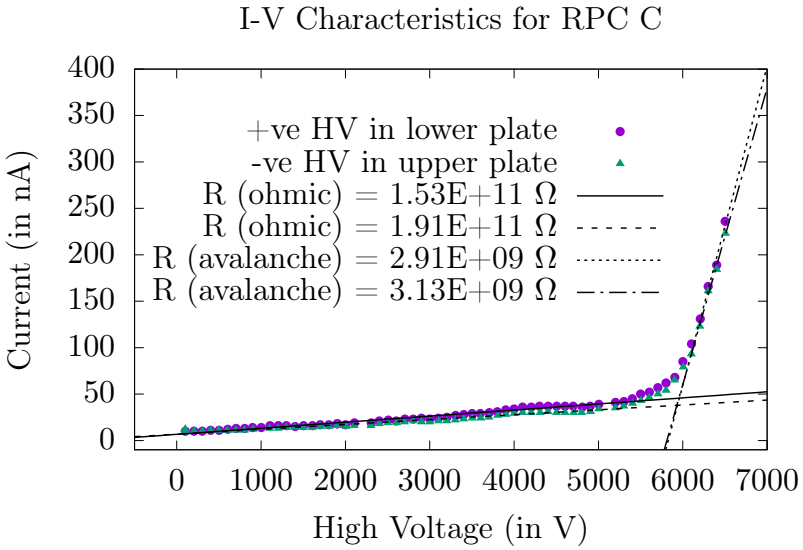

Figure 3.20: I-V Characteristics of RPC C

top panel had been provided with positive high voltage so the pickup strips give a negative pulse. The RPCs were arranged in stack with the order from top to bottom as RPC A, RPC B, and RPC C. The first finger paddle was placed on top of RPC A, Second paddle was placed on top of RPC C and the third paddle is placed below the RPC C. All the paddle were required to be aligned with the third strip of top pickup panel (positive electrode).

The three scintillator paddles formed the trigger. The trigger signal ensured that the muon was passed through all the three paddles. The three-fold coincidence had been taken between the three paddles. To find the efficiency

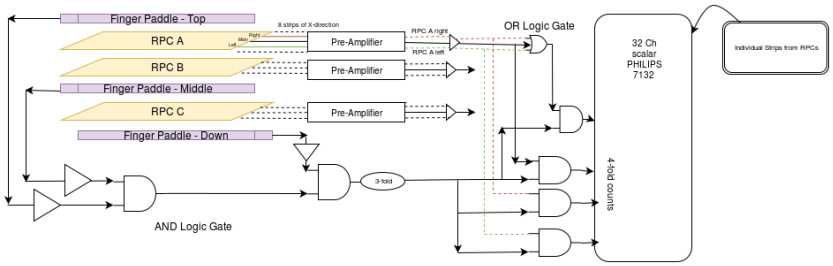

Figure 3.21: Experimental setup for characterization of RPC

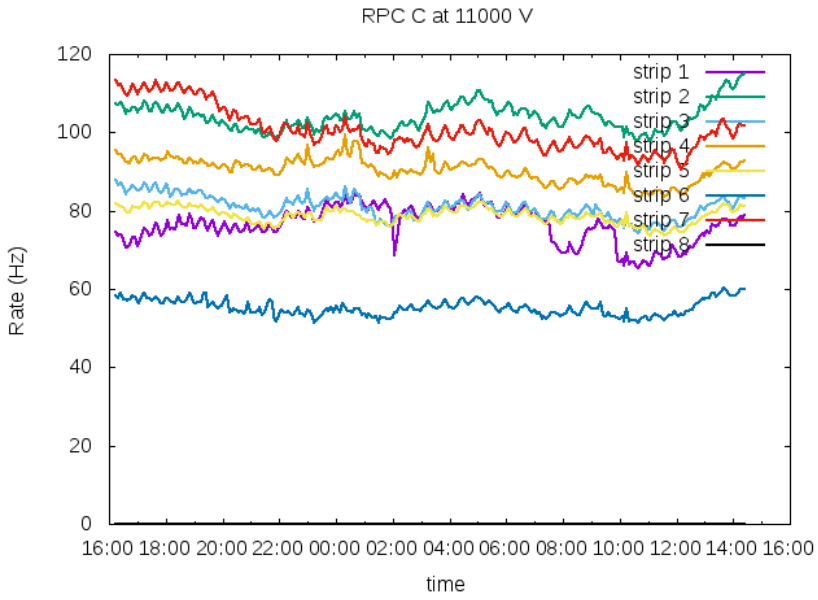

Figure 3.22: Count rate of various strips of RPC C at 11000 V

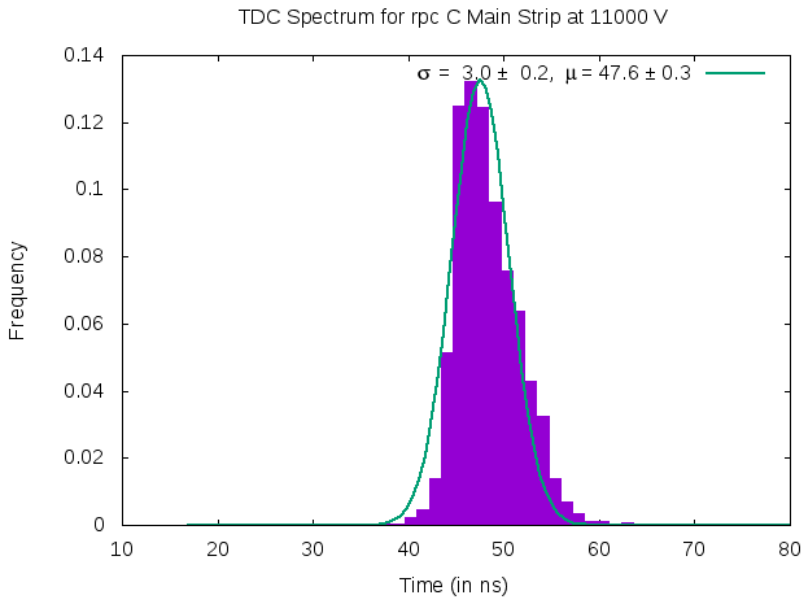

Figure 3.23: TDC spectrum of Main (3rd) strip of RPC C at 11000 V

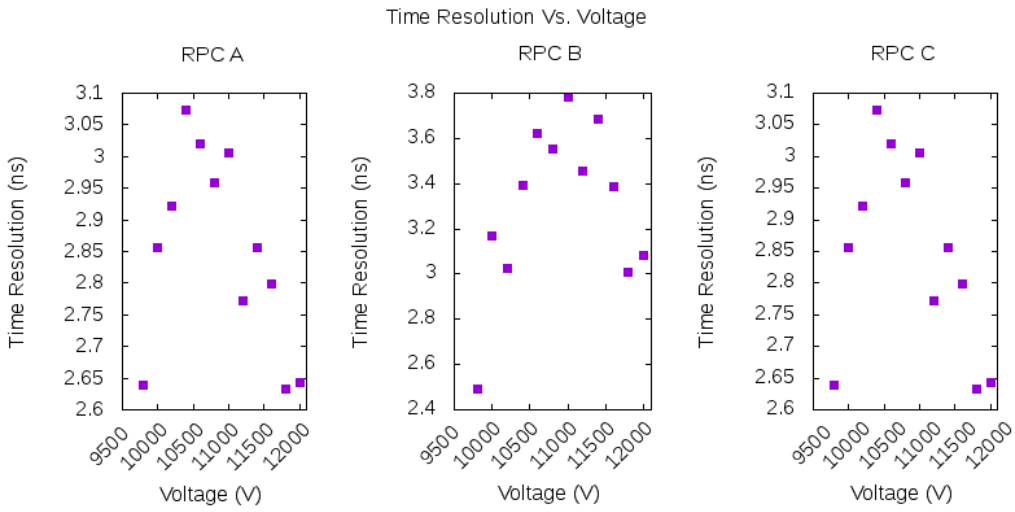

Figure 3.24: Variation of Time Resolution with applied High Voltage for all the RPCs

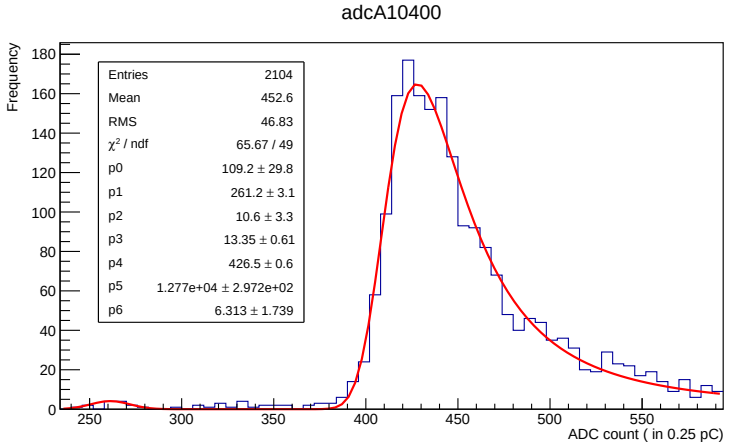

Figure 3.25: ADC spectrum of Main (3rd) strip of RPC A at 10400 V

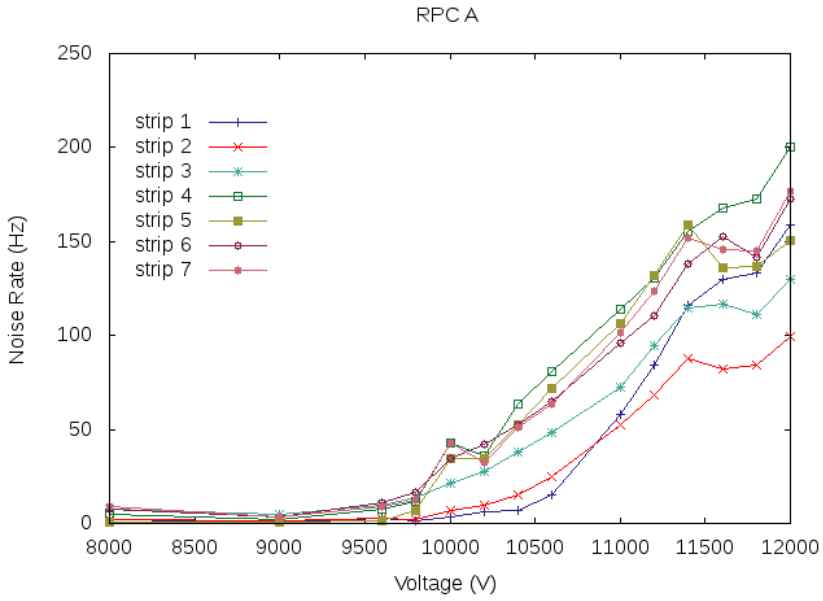

Figure 3.26: Noise Rate of RPC A

of a strip, we needed to make coincidence between trigger and strip signal which was actually a four-fold coincidence. The efficiency of the strip was given by

$$\text{Efficiency} \quad = \quad \frac{\text{Four fold Rate}}{\text{Three fold Rate}}, \tag{3.3}$$

We measured efficiency of the third strip, left strip, right strip and OR of these three strips.

The efficiency for RPC A, RPC B and RPC C are shown in Figures 3.27, 3.29 and 3.31 respectively. Figure 3.33 shows the comparison of efficiency for RPC A, RPC B and RPC C. We can see that the efficiency increased with applied voltage and saturated at high voltage which can also be called Plateau region. In the plateau region, the efficiency became independent of applied voltage. The operating voltage of RPC should be a start point of the plateau region.

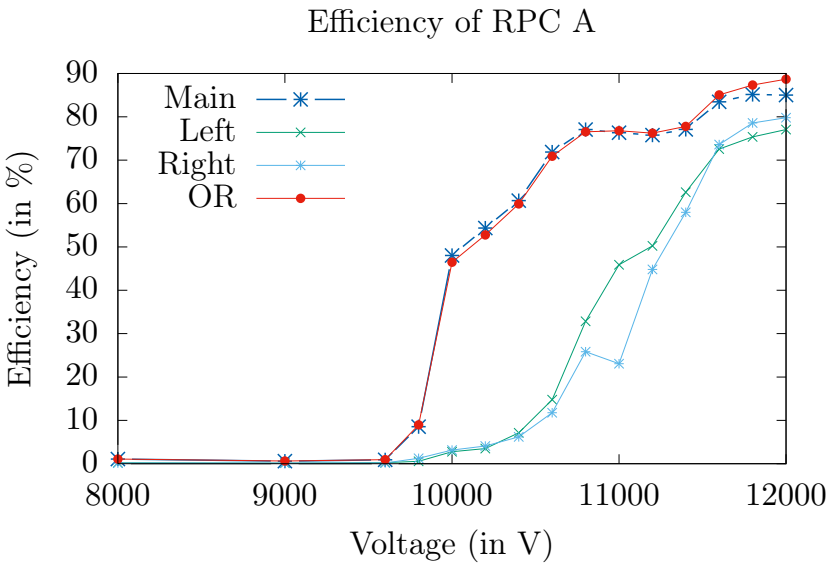

Figure 3.27: Efficiency of RPC A

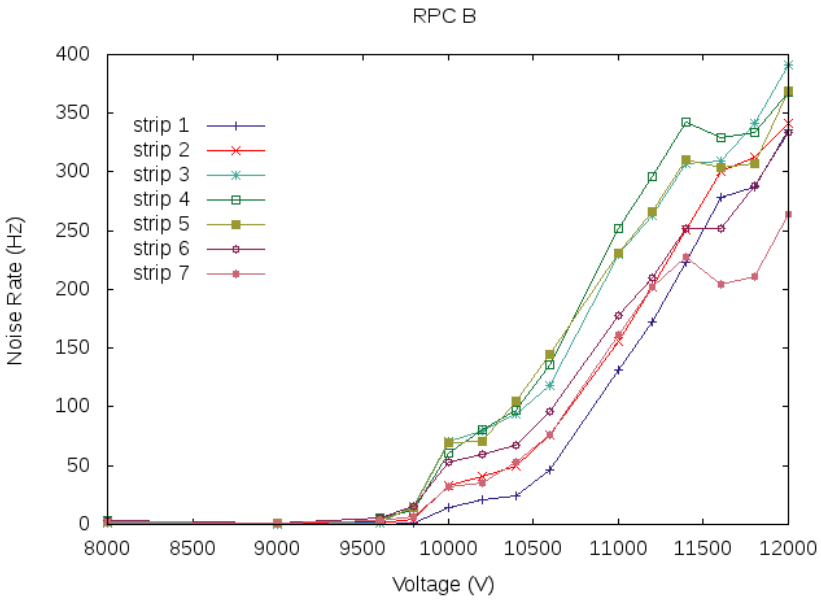

Figure 3.28: Noise Rate of RPC B

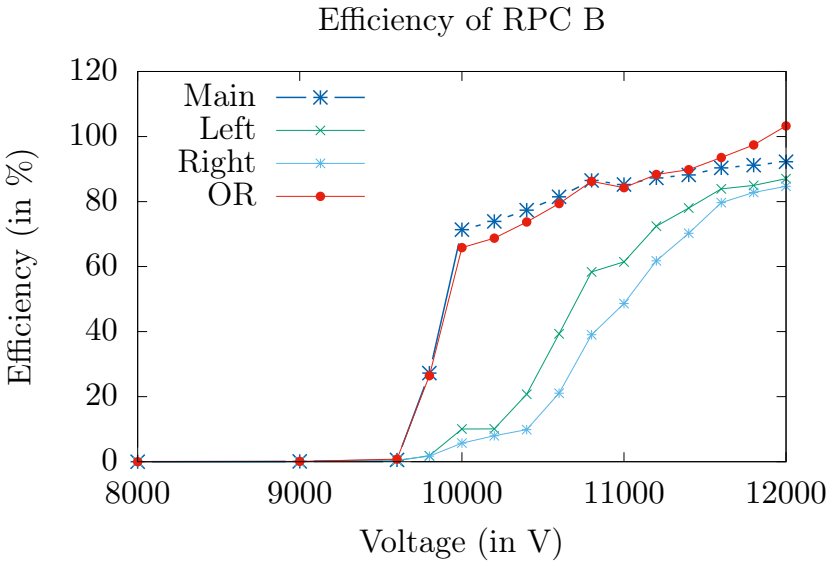

Figure 3.29: efficiency of RPC B

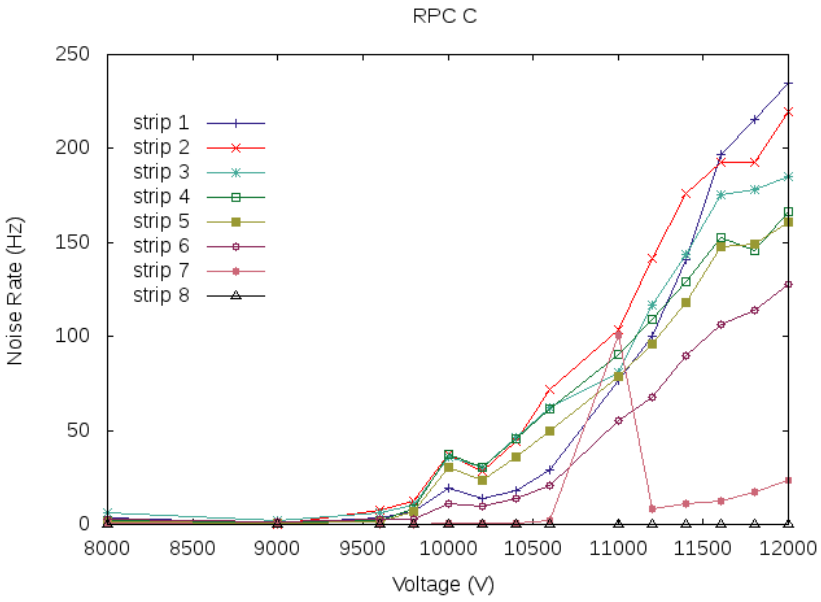

Figure 3.30: Noise Rate of RPC C

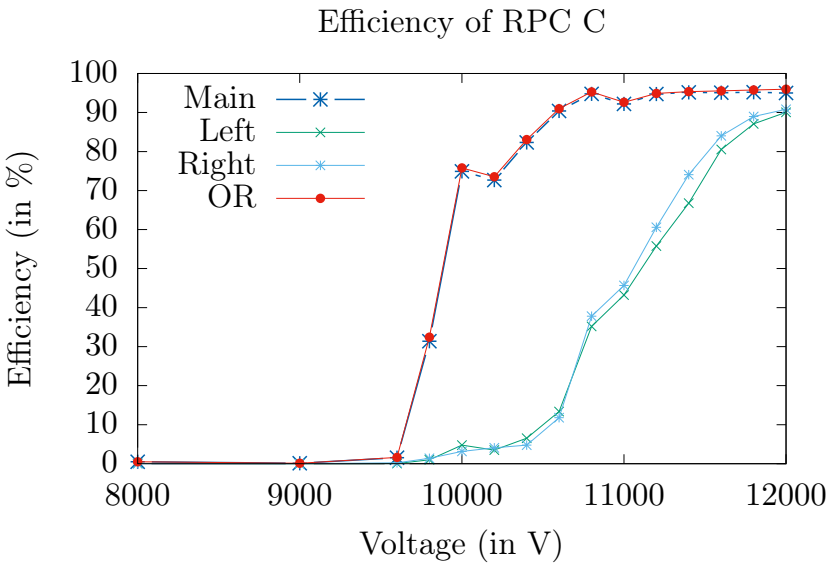

Figure 3.31: efficiency of RPC C

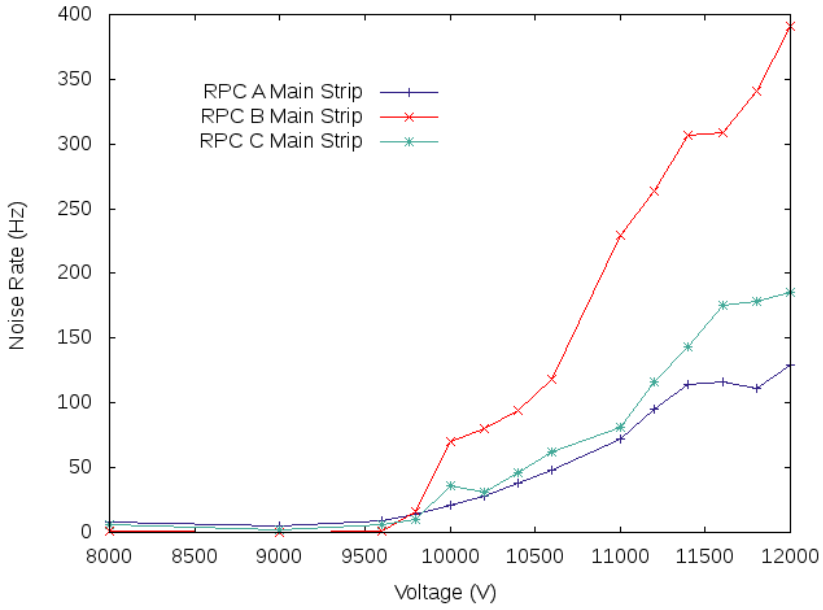

Figure 3.32: Comparison of Noise Rate of Main strip (3) of all three RPCs

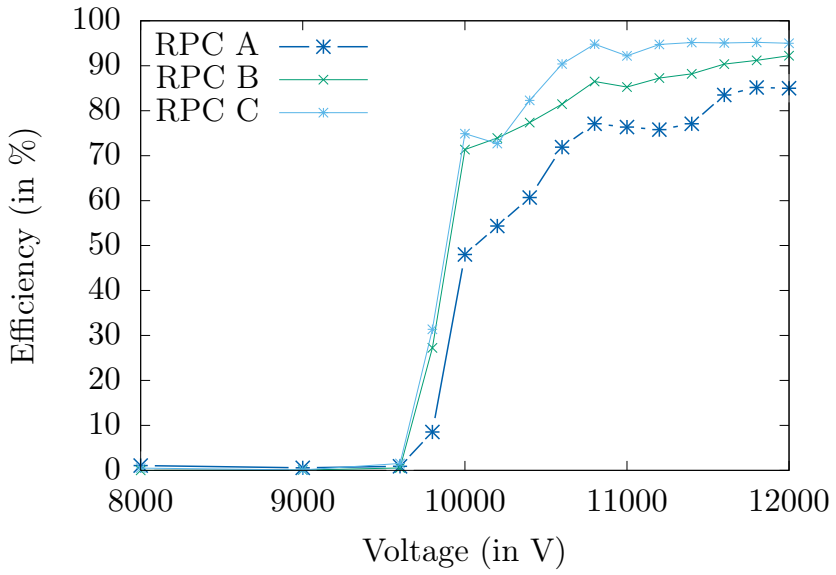

Figure 3.33: Comparison of efficiency of Main strip (3) of all three RPCs

Bibliography

[1] Dr. William R.Leo. Techniques for Nuclear and Particle Physics Experiments. Springer, 2nd edition, 2013.

[2] Glenn F. Knoll. Radiation Detection and Measurement. Wiley India Pvt. Ltd., 3rd edition, 2009.

[3] Christian Lippmann. Detector Physics of Resistive Plate Chambers. PhD Thesis, 2003.

[4] B. Satyanarayana. Design and Characterization Studies of Resistive Plate Chambers. PhD Thesis, Indian Institute of Technology Bombay, India, 2009.

[5] P.Fonte. Applications and new developments in Resistive Plate Chambers. IEEE Trans. Nucl. Sci. 2001.